

## FRICION IMPROVEMENT VIA GRINDING WHEEL TEXTURING BY DRESSING

Maria Garcia Moreno <sup>a,\*</sup>, Jorge Álvarez Ruiz <sup>a</sup>, David Barrenetxea Azpeitia <sup>a</sup>,  
Jose Ignacio Marquín González <sup>a</sup>, Leire Godino Fernández <sup>b</sup>

<sup>a</sup> IDEKO S.Coop, Arriaga Kalea, 2, 20870 Elgoibar, Gipuzkoa, Spain.

<sup>b</sup> Faculty of Engineering Bilbao, University of the Basque Country (UPV/EHU), Plaza Torres  
Quevedo, 1, 48013 Bilbao, Spain

\*Corresponding author. Tel: +34 943748000. mgarcia@ideko.es

---

### Abstract:

The economic and environmental cost of friction in machinery and transport is significantly remarkable being the machine tool one of the most affected. In this sector, the movements are fully affected by the friction originated in the displacements between the guideways and the slides, which results in terms of precision, energy consumption and component deterioration. In this line, texturing has proved to be a useful tool to lessen friction. Nowadays, flaking is the technique in use for the texturing of machine tool guideways, a manual and costly process in which the final finish of the workpiece is not controllable. Other techniques like laser texturing constitute an effective and precise procedure which is at the same time and cost expensive, requires fine tuning of process parameters and is not applicable in large workpieces. Therefore, the main challenge is to develop an industry implemented technique capable of producing textures in a repetitive and economically viable way. In this work, a method that allows generating a wide range of controlled textures by grinding with wheels textured with an assisted dressing device, is presented. With this technique it is possible to create textures in large workpieces, such as machine tool guideways and to do it in a repetitive way and in the same machine in which the guide has been ground previously, which involves a reduction in time and costs. The technique has been validated by means of tribological tests in which textures generated with this technique have obtained lower friction coefficients than flaking.

---

**Keywords:** Friction, grinding, texturing, dimples, machine-tool, guideways.

---

# 1. INTRODUCTION

Friction is the resistance force to the relative sliding of a solid over another. Friction is always present, although a fluid or solid lubricant is put in between the surfaces to eliminate it. Nowadays, friction is one of the main concerns in manufacturing and industries such as automotive and equipment goods are heavily investing in research on how to reduce friction and wear in mechanical systems [1-5]. The results of tribology studies show that by taking advantage of the new surface, materials, and lubrication technologies for friction reduction and wear protection in vehicles, machinery and other equipment worldwide, energy losses due to friction and wear could potentially be reduced by 40% in the long term and by 18% in the short term [6].

One of the most important fields affected by friction is machine tools. In this sector, movements are fully influenced by the friction originated in the displacements between guideways and slides surfaces. This influence comes in terms of accuracy of movements, as well as power consumption and wear of sliding parts. As a key component of machine tools, sliding guideways are required to have high guidance precision, good wear resistance, low speed stability, and high contact stiffness, which affects the machining accuracy and service life of the machine tool [7]. In general, wear and contact fatigue, which are greatly impacted by friction properties of the contact surfaces, are the most common failure modes for guideways. It is well-known that the lubricating property would be improved when friction force decreases in the same load.

Nowadays, the industrial approach to reduce the friction, lies in the combination of the use of a polytetrafluoroethylene PTFE polymer layer in moving slides surfaces, and the scrapping [8] and flaking of the cast iron surface of the static guideways, as well as the lubrication by means of a suitable oil. Although the main objective of scrapping is to reduce the surface roughness and improve the contact between two surfaces [9], by means of flaking what it is attempted to do is to create shallow forms on the sliding surface (Fig 1), that can act as lubricant deposits and that way ensure the presence of lubricant in the contact zone at all times, reducing the friction and wear during the relative movement [10]. It is a surface finishing method that is done removing thin chips from the surface by means of a metallic tool with a carbide point and that must be carried out on previously machined surfaces. As a result, friction is kept in low values, sliding problems like stick-slip are avoided and working life of sliding guideways surfaces is prolonged. However, flaking is a laborious work that requires significant experience on the part of the operators. Moreover, being a manual operation, it is an uncontrolled, cost-un-effective and time-consuming process. In the present day, this manual operation has poor indicative validation parameters set when it comes to the shape of the print, orientation of it and percentage of print versus total surface, but no qualitative measuring of the geometry of the obtained surface is done, neither of its tribological capacity. An improperly conducted scrapping operation can generate scratches and surface damage [11], which seriously affects the performance of the guide rail and the machining accuracy.

To avoid flaking drawbacks, the alternative of surface texturing for implementing different patterns on the guideway surfaces arises. Such patterns can act as reservoirs for lubricant and be effective for obtaining desirable friction or fluid flow characteristics. Besides, in many situations, the wear between two sliding surfaces can be reduced via surface texturing by avoiding the presence of debris, which originates the abrasive wear of the sliding components, as it is entrapped inside the pockets that compose the texture [12-14]. A considerable research work on surface texturing has been carried out with this purpose. In 2008, Bruzzone et al. [15] proposed the following categorization for the manufacturing methods used for surface texturing based on the physical principles involved: adding material, removing material (ex.: laser methods, etching, micro cutting, grinding), moving material (ex.: shot blasting) and self-forming. A review on some of these different techniques and different texture patterns is developed below.

Previous research developed by Costa and Hutchings [16] showed that the use of small cavities uniformly distributed over the sliding surface offers the best tribological results for hydrodynamic bearings. In 2009

and 2010 Galda et al. [17-18] studied the influence of different shapes and arrangements of oil pockets on friction and their effects on seizure resistance of steel bearings. Pockets were manufactured by burnishing, tribological tests showed improvement of seizure behaviour in texturized surfaces furthermore shape demonstrated to be the main factor in this improvement. The work developed by M. Nakano et al. [19] compared micro-texturing by shot blasting on masked cast iron surfaces of 6-10  $\mu\text{m}$  depth 60  $\mu\text{m}$  diameter, to milled grooves of 40-50  $\mu\text{m}$  depth 500  $\mu\text{m}$  diameter and flat surfaces. Grooved patterns suppressed the generation of hydrodynamic pressure resulting in higher friction. Micro dimple pattern increased load carrying capacity of lubricant film, leading to lower friction.

Current approaches to produce functional surfaces include, but are not limited to etching, lithography and laser machining. A. Kovalchenko et al. [20] used laser for micro texturing, generating 4-6 $\mu\text{m}$  depth 58-80  $\mu\text{m}$  diameter dimples on hardened steel. Pin-on-disc tribology tests showed to expand the range of the hydrodynamic lubrication regime in terms of load and sliding speed as well as the reduction of the friction coefficient, concluding that a lower dimple density was more beneficial for lubrication. Laser texturing is an efficient and precise procedure but at the same time it has a low-production rate and it is not applicable to large workpieces. Besides it requires fine tuning of process parameters to control metal recast, high hardware investment as well as more complex operational training and safety requirements. Alternatives for producing functional surfaces using traditional machining processes are presently sought.

Therefore, the challenge is to develop an industry implemented process to produce textures at a low cost and feasible cycle times and with a certain degree of flexibility when it comes to the textures that can be generated in terms of shape, size and distribution. Thus, the option of texturing by grinding arises as a potential alternative by combining its inherent finishing process characteristics, its cost effectivity and easily controlled process parameters. Another favourable point is that, by grinding, texturing could be implemented in any kind of surface, regardless of the part material, from small lengths of 10-20 mm to larger ones of 12-18 meters. In the case of the industrial manufacturing of the guideways, texturing by grinding presents also the advantage that grinding is already part of guideways manufacturing process; therefore, no additional investment should be necessary, operation costs would not be increased significantly. Another fact to take into consideration is that grinding is a fully automatized and controlled process, so when grinding is used for texturing, actual manual, uncontrolled, cost non-effective, and tedious operation for workers, which is flaking, is made redundant. In addition, this change from manual to fully automatized process is translated into a considerable time reduction.

The techniques of texturing by grinding have evolved through history, it was first introduced by CIRP researchers [21], with a method based on grinding by wheels with helical patterns created by single point dresser using special dressing parameters, which was applied to ceramic bearings. Research results on process modelling, simulation and experiments were shown in subsequent works [22-26]. In 2009 Denkena et al. [27] proposed a new strategy to obtain micro profiles on the grinding wheel surface. In this case, dressing is carried out by profiled dressing discs. This method is more stable and efficient than single-point or roll dressing. The technique was applied for implementing micro-grooves in compressor blades in order to reduce friction on turbulent flow. In the continuation of the study [28] friction reductions of up to 4% are found. In 2010, Denkena et al. [29] used normal cutting operations such as turning and milling as well as abrasive processes such as grinding to apply geometric patterns or pockets in large areas. Using both processes a large flexibility and high precision was achieved. Oliveira et al. presented another technique to texturize the grinding wheel surface by continuous modification of dressing depth [30-31] by connecting the dresser to a dispositive. The span of textures that can be achieved is increased as it is shown in different study cases.

This paper presents an industrial solution to lessen friction on cast iron guideways surfaces. This friction reduction will be achieved by a grinding for texturing approach. Texturing should be implemented on surface wheel by a dressing operation carried out by an assisted dressing tool. The dressing device developed based on the concept presented by Oliveira in [30], as well as the procedure used to texture, and the advantages and disadvantages of the different texture patterns evaluated by means of tribology tests are

shown in the present document. Finally, the conclusions of the research, as well as further work to be developed will be reported.

## 2. DEVELOPMENTS

### 2.1. Purpose-built assisted dressing device

A purpose-built assisted dressing device has been conceived in order to have a technology to generate defined patterns on the surface of the grinding wheel by means of the dressing operation.

Based on the concept presented by Oliveira et al. [30], the methodology of application of this technology is based on the generation of signals from a device which are sent to the piezoelectric actuator, which actuates on the dresser, providing it with a controlled penetration movement during the dressing process. By adjusting correctly, the dressing feed rate, the wheel speed and the input signals, it is possible to generate different types of patterns on the wheel surface. These patterns will be later copied on the surface of the ground workpiece, generating functional surfaces depending on the patterns generated on the wheel and the used grinding parameters.

For the design of the tool where the piezoelectric actuator and the dresser must be assembled, dynamic and stiffness calculus have been carried out. Aluminium has been selected to build the tool because of its fatigue behaviour is better than that of the steel. Size of the tool has been defined keeping in mind the need to host all the cables, the piezoelectric actuator and the refrigeration of the inside of the device, which is done with compressed air, but without losing sight of the space available inside the machine where the device will be installed, otherwise, collision problems could arise. Another key aspect is the water-tightness of the device, since both dressing and grinding are performed under lubricated conditions. Thus, special care has been taken that none of the edges communicates directly with the exterior and that two sealing rings can be fitted in the mobile part in order to prevent coolant from getting inside the device. Besides, the compressed air that is used for refrigeration, generates a positive internal pressure that prevents the entrance of coolant. Considering this all, the general dimensions of the designed tool are 92 x 94 x 84 mm (Fig 2a). Finally, prior to building the tool and testing its proper functioning in the machine, the validation of the performance of the design against the forces generated during the dressing process has been done by means of a FEM analysis.

The device is a system composed by the elements shown in Fig. 2b:

- A piezoelectric actuator placed on the single-point dresser.
- A device to generate the input signals for the actuator.
- A software to generate the signal depending on defined dressing conditions and the surface to be obtained on the final workpiece.

### 2.2. Theoretical analysis

The proposed scheme, in which the user defined patterns can be imprint on the wheel surface during dressing and later transferred to the part, promotes a freedom of choices for transferring patterns to the workpiece during grinding. The shape, the size and the depth of the dimples, their distribution and the density of the texture on the workpiece surface are the different parameters to be defined.

The distribution of the texture affects the friction coefficient and so, with the objective of keeping it constant during the whole displacement of the slides along the guideways, the defined texture has a distribution that ensures that the proportion of texture on the contact surface is kept constant. Besides, a transversal overlapping has been defined to ensure that the slides will always find a lubricant housed inside the dimple which they can drag to the non-textured zone, create a lubricant film between the surfaces and diminish the friction between the guideway and the slide.

The width of the dimple generated on the textured surface is the same as the width of the dimple generated on the wheel by means of the assisted dressing tool. The minimum dimple width that can be generated on the wheel, and so on the textured surface is limited by the response speed of the piezoelectric actuator and the dressing transversal speed. The maximum width is limited by the wheel width and the number of dimples that the user wants to fit into it.

The length of the dimple which is obtained as a result on the workpiece ( $l_{dimp}$ ) depends on different factors: the contact length, the length of the dimple generated on the grinding wheel with the assisted dressing ( $p_{dimp}$ ) and the grinding feed rate ( $v_w$ ). Discretizing the perimeter of the grinding wheel in points ( $p_{rev}$ ), the length of the dimple that will be generated on the surface of the workpiece can be calculated in the following way:

$$l_{dimp} = 2 \cdot \sqrt{d_s \cdot a_e} + \frac{p_{dimp}}{p_{rev}} \cdot v_w \quad (2.1)$$

The contact length is the trajectory that each point of the periphery of the wheel describes on the workpiece and that varies depending on the grinding pass depth ( $a_e$ ) for a given wheel diameter ( $d_s$ ). The greater the grinding pass depth, the greater the length of the dimple generated on the guideway. Besides, the grinding pass depth defines the depth of the dimple generated on the guideway. However, it must be considered that this depth is limited by the height of the dimple generated on the wheel with the dressing, which corresponds to  $a_d$ . If the grinding pass depth is equal or greater than the wheel dimple height, when grinding the guideway, the non-textured part of the wheel will also be grinding and so, the depth of the dimple that will be obtained on the guideway will be equal to the height of the dimple on the wheel. In the same way, the length of the dimple which depends on the contact length will also be limited in this way.

When it comes to the length of the dimple generated on the wheel, this depends on the input signal sent to the assisted dresser, in which the time during which the dresser must retreat (must penetrate less on the wheel) in order to create the texture is defined. Finally, a higher or lower grinding feed rate results on the generated dimples being longer or shorter respectively. In addition, it also defines the longitudinal distance between the textures generated by the same wheel dimple. For a higher or lower grinding feed rate the spacing will be greater or smaller respectively, achieving like this a greater or lower density of dimples.

The following diagram is shown as a summary of the influence of the length of the wheel dimple and the grinding feed rate (Fig. 3). It shows that for a given feed rate, the longitudinal distance between dimples is the same, but that depending on the length of the dimple generated on the wheel with the dressing the superficial area of texture can be higher or lower. Equally, if the feed rate varies for a given wheel texture, the longitudinal distance between dimples changes but also does their length (as showed in equation 2.1).

### 2.3. Texture generation and simulation model

Taking all the parameters that have been analysed in the previous theoretical analysis into consideration, a model has been developed with the objective of automatizing the process of texturing by grinding. The model is capable of creating an input signal for the piezoelectric actuator in order to create the texture on the grinding wheel by dressing and then provide the suitable grinding parameters to be used in order to obtain the desired texture on the guideways. In general terms, the model works in the following way:

First, the dimensions of the contact area and the percentage of non-textured surface are defined. This proportion is kept constant in the whole length of the guideway. The size of the dimple in terms of length ( $l_{dimp}$ ), width ( $w_{dimp}$ ) and depth ( $a_{dimp}$ ) needs to be defined as well.

The next step is to select the proper dressing parameters based on the desired output and the dresser characteristics. Once this is defined, it is possible to calculate the texture needed on the grinding wheel.

With the calculated grinding wheel texture, the input signal for the assisted dresser is created. The signal is represented as a matrix of dimensions *wheel perimeter*  $\times$  *wheel width* which represents the surface of the wheel (Fig. 8). On this surface a single dressing stroke of  $a_d$  is performed except on the areas where the assisted dresser must retreat  $a_d$  in order to create the textures.

This signal is then loaded on the software developed for the application, in which the characteristics of the piezoelectric actuator that is going to be used are set. In this manner, input signal is translated into the voltage to be commanded to the piezoelectric in every instant. This voltage signal is the one that controls the greater or smaller penetration of the dresser on the grinding wheel, generating this way the texture. During dressing with the aim to control the length ( $l_{dimp_s}$ ), width ( $w_{dimp_s}$ ) and depth ( $a_{dimp_s}$ ) of the dimples that are being generated on the wheel, the real voltage signal of the piezoelectric is acquired in order to compare it with the one commanded by the software.

Once the grinding wheel is dressed, the next step is to transfer the wheel pattern to the workpiece. The grinding parameters to be used in order to achieve the texture characteristics set in the first step (Fig. 4) are calculated.

- $a_e = a_{dimp}$  (2.2)

- $N^{\circ} \text{ strokes} = 1$  (2.3)

- $n_s = n_{sd}$  (2.4)

- $v_w = n_s \cdot (l_{dimp} - 2 \cdot \sqrt{d_s \cdot a_e}) \cdot p_{rev} / p_{dimp}$  (2.5)

Toward facilitating the texture generation process, the model is able to simulate the textured part surface that will be obtained by using the given wheel texture and grinding parameters (Fig. 8), so the user can see an estimated result prior to performing it experimentally. The simulation takes into account the shape of the wheel generated by means of the assisted dressing device and simulates the trajectory that each point of the periphery of the discretized wheel makes on the surface of the guideway.

### 3. EXPERIMENTAL VALIDATION

Next, the results obtained from the generation of textures using the model developed in the previous section, as well as the results of the friction coefficients obtained in the tribological tests for each texture. The work has been developed in a Danobat DS-630 machining centre (Fig. 9a), a Norton grinding wheel of 320 mm in diameter and a single point dresser with an effective width of 0.8 mm (Fig. 9b). A water-based coolant from Castrol has been used for both dressing and grinding operations.

For the validation of the texturing technique all generated textures have been measured with a confocal microscope (Fig. 9c) and finally, tribological tests have been performed in order to compare the friction coefficients of each texture against that of the flaked surfaces.

#### 3.1. Test part design

To simulate the functioning of the guideways and slides of the machines and taking into account the characteristics of the tribometer in which the tribological test will be performed later, two types of test parts have been designed:

- Mini-guideway: GG30 test part with a surface of 64 x 40 mm on which the textures are generated by grinding.
- Mini-slide: test part composed of a GG30 square body on whose 30 x 30 mm surface a layer of turcite of 3 mm thickness is glued.

### 3.2. Previous grinding of test parts

Before generating the textures on the surface of the mini-guideways it is necessary to grind both the mini-guideways and mini-slides in order to obtain the superficial tolerances ( $R_a = 0.8 \mu\text{m}$ ) required to this type of surfaces. To do so, all the surfaces have been ground with parameters similar to those used nowadays in the grinding of the real guideways and slides, which are shown on Table 1. With these conditions a  $R_a = 0.42 \mu\text{m}$  and  $R_z = 2.13 \mu\text{m}$  have been obtained in transversal direction.

	Usual conditions	Tests by Ideko
<b>Grinding wheel</b>	High-porosity Wheel, coarse grain size 46-60 and low hardness F-H.	Norton Vortex IP A60F.H 26VTX2
<b>Cutting speed (m/s)</b>	25-35	33
<b>Feed rate (mm/min)</b>	15000-25000	9390
<b>Grinding pass (mm)</b>	0,005	0,005
<b>Sparkout strokes</b>	2-4	4
<b>Dressing feed rate (mm/min)</b>	120-240	200
<b>Dressing strokes</b>	2x0,02	2x0,02

*Table 1. Dressing and grinding conditions for the previous grinding of test parts.*

### 3.3. Texture generation and tribological tests

With the objective of analysing the influence of the different textures on the friction coefficient and compare them to the flaking two series of textured test parts have been done and tribological tests have been performed on them as it follows.

The friction tests have been performed on a UMT-3 tribometer. The samples are mounted in pairs, one miniguide and one mini-slide. During the tests, the miniguide is fixed and the mini-slide moves to simulate the relative movement between the machine guideway and slide (Fig. 10). The linear oscillating movement of the mini-slide has a displacement  $d$  of 10 mm and a frequency  $f$  of 0'1, 1, 7'5 y 15 Hz. The linear velocity is continuously variable in the cycle, but  $V = 2 \cdot d \cdot f$  is taken as representative value, which means speeds range between 120 and 18000 mm/min, which are the speeds at which machine guideways work.

#### 3.3.1. First series

The first series of tests is divided into two parts, the first one compares the frictional behaviour of a flaked surface with a textured surface under different loads. The second, compares a flaked surface with different textures.

In the first part of this series the frictional behaviour of a flaked surface has been compared to that of a texture of spherical dimples of  $8 \mu\text{m}$  in depth ( $a_{dimp}$ ) and 4 mm in diameter ( $\emptyset_{dimp}$ ). The average friction coefficients obtained from the tribological tests performed for each type of surface are shown in Fig. 11.

It is possible to observe that the speed of displacement of the slides has influence on the friction coefficient. In the case of scrapped surfaces, the friction coefficient increases as the speed increases. For the textured surface instead, the friction coefficients decrease as speed increases.

Comparing the friction values of the flaked surface the textured surface, it is evident that even though the friction values are similar for low displacement speeds, as the speed increases the friction coefficient difference is more significant. Looking at the influence of the load applied to the slide in the friction values, it is possible to see that friction values are a bit lower for both flaked and textured surfaces when the applied load is higher. Friction coefficient reductions obtained with texture A with respect to the flaked surface, for both loads of 18 and 36 kg, are shown in table 2.

FRICTION COEFFICIENT REDUCTION (%)		
	Texture A 18 kg	Texture A 36 kg
0,1 Hz	0	27
1 Hz	13	29
7,5 Hz	68	70
15 Hz	75	68

Table 2. Friction coefficient reductions texture A vs flaked surface.

Considering the results obtained in the first part of this series, the second part focuses on comparing textures with different characteristics (Table 3) to a flaked surface. Texture A is the one used in the first part of trials of this series, texture B has a higher density of texture due to a higher trasnversal overlapping of the dimples and texture C has a higher density of texture due to a shorter distance between dimples in the grinding direction ( $d_{dimples}$ ) wich is obtained by decreasing the grinding feed rate.

TEXTURED SURFACE CHARACTERISTICS		
Texture A	Texture B	Texture C
$a_{dimp} = 8 \mu\text{m}$ $\varnothing_{dimp} = 4 \text{ mm}$ overlapping = 48% $d_{dimples} = 4.5 \text{ mm}$	$a_{dimp} = 8 \mu\text{m}$ $\varnothing_{dimp} = 4 \text{ mm}$ overlapping = 72% $d_{dimples} = 4.5 \text{ mm}$	$a_{dimp} = 8 \mu\text{m}$ $\varnothing_{dimp} = 4 \text{ mm}$ overlapping = 48% $d_{dimples} = 4 \text{ mm}$

Table 3. Characteristics of textured surfaces.

The average friction coefficients obtained from the tribological tests performed for each type of surface are shown in Fig 12.

In the same way as in the previous tests, it is clear that the friction coefficients of the fleaked surface increase with the speed of displacement of the slide and the for the textured surfaces the friction coefficients decrease instead. Comparing the different textures to the flaked surface, all of them show a reduction of the friction coefficient which is especially notorious at high displacement speeds. Texture B is the one with the greatest friction reduction for all the displacement speeds. This means, that for the same size and depth of dimple, a higher transversal overlapping of the texture is beneficial. Texture C, with the same transversal overlapping as texture A, but with a shorter distance between dimples in the grinding direction, which translates in a higher texture density as well, shows a higher reduction of the friction coefficients. Table 4 shows the friction coefficient reductions of the different textures respect to the flaked surface.

FRICTION COEFFICIENT REDUCTION (%)			
	Texture A	Texture B	Texture C
0,1 Hz	0	29	29



<b>1 Hz</b>	13	33	27
<b>7,5 Hz</b>	68	77	64
<b>15 Hz</b>	75	75	75

Table 4. Friction coefficient reductions of textures A, B and C with respect to the flaked surface.

### 3.3.2. Second series

For the second series of test a preliminary characterization of the flaked surfaces has been done. In Fig. 13a and Fig. 13b the topography of the flaked surface measured by means of the confocal microscope is shown. In the A profile extracted from the measurement it is possible to see that the mean depth of the grooves is of 12  $\mu\text{m}$  approximately (Fig. 13c). In the B profile, it is possible to see that the mean width of the biggest zone of the half-moon shapes created by flaking is of about 4 mm (Fig. 13d). Applying the Abbott Firestone curve to the surface it has been observed that it has a 25% of non-textured surface against total surface.

Based on the results obtained from the first series and the results of the characterization of the flaked surface the textures shown in Table 6 have been defined. A base texture has been set which has a dimple depth of 12  $\mu\text{m}$ , width of 3.7 mm and a 25 % of non-textured surface versus total surface in order emulate the flaked surface. The transversal overlapping of the dimples has been set as 72 % as in texture B. Starting from this, five other textures have been generated with different dimple depths and texture densities in order to study the influence of these two characteristics on the friction coefficient.

For all the cases the wheel has been dressed with the following conditions:  $n_{sd} = 1800$  rpm,  $a_{vd} = 0.1$  mm/rev and  $a_d = 25$   $\mu\text{m}$  and single grinding stroke has been done with the conditions showed in Table 5.

GRINDING CONDITIONS		
T1	T2	T3
$a_e = 12 \mu\text{m}$	$a_e = 12 \mu\text{m}$	$a_e = 12 \mu\text{m}$
$n_s = 1800$ rpm	$n_s = 1800$ rpm	$n_s = 1800$ rpm
$v_w = 9028 \frac{\text{mm}}{\text{min}}$	$v_w = 12352 \frac{\text{mm}}{\text{min}}$	$v_w = 19923 \frac{\text{mm}}{\text{min}}$
T4	T5	T6
$a_e = 8 \mu\text{m}$	$a_e = 8 \mu\text{m}$	$a_e = 8 \mu\text{m}$
$n_s = 1800$ rpm	$n_s = 1800$ rpm	$n_s = 1800$ rpm
$v_w = 9000 \frac{\text{mm}}{\text{min}}$	$v_w = 12273 \frac{\text{mm}}{\text{min}}$	$v_w = 19919 \frac{\text{mm}}{\text{min}}$

Table 5. Grinding conditions for textures of the second series of tests.

The topography of the resulting surface for each of the mini-guides has been measured using the confocal microscope. The profile of the surface has been extracted from the measured topography and the width, length and depth of the dimples have been measured and verified to coincide with the defined. Moreover, applying the Abbott Firestone curve the proportion of non-textured surface has been verified to be quite similar to the defined. This way, the obtained results (Table 6) have been useful to validate the texture generation and simulation model.

Texture nr.	Texture desired on the contact surface	Texture validation (topography obtained with the confocal)
-------------	--	--

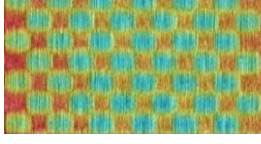

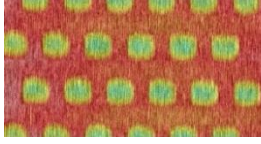
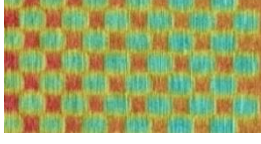
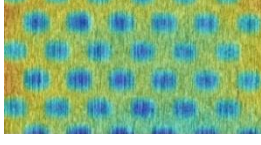
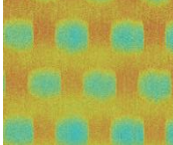
<b>T1</b>	$a_{dimp} = 12 \mu m$ $perc = 25\%$		$a_{dimp} = 10 \mu m$ $perc = 23.15\%$ $w_{dimp} = 3.7 \text{ mm}$
<b>T2</b>	$a_{dimp} = 12 \mu m$ $perc = 45\%$		$a_{dimp} = 11 \mu m$ $perc = 47.99\%$ $w_{dimp} = 3.7 \text{ mm}$
<b>T3</b>	$a_{dimp} = 12 \mu m$ $perc = 66\%$		$a_{dimp} = 11 \mu m$ $perc = 69.20\%$ $w_{dimp} = 3.7 \text{ mm}$
<b>T4</b>	$a_{dimp} = 8 \mu m$ $perc = 25\%$		$a_{dimp} = 8 \mu m$ $perc = 20.68\%$ $w_{dimp} = 3.7 \text{ mm}$
<b>T5</b>	$a_{dimp} = 8 \mu m$ $perc = 45\%$		$a_{dimp} = 8 \mu m$ $perc = 44.58\%$ $w_{dimp} = 3.7 \text{ mm}$
<b>T6</b>	$a_{dimp} = 8 \mu m$ $perc = 66\%$		$a_{dimp} = 8 \mu m$ $perc = 63\%$ $w_{dimp} = 3.7 \text{ mm}$

Table 6. Characteristics of the desired part texture and texture validation results.

The results of the tribological tests performed for the second series of textures are shown in Fig 14. In it, it is possible to observe that all the textures present lower friction coefficients, in a higher or lower degree, than the flaked surface for all the four movement frequencies that have been analysed.

Comparing the behaviour of the flaked miniguide with the base texture (T1), it is possible to see that for low frequencies the friction coefficient is quite similar, however, as frequency increases, so does the difference between the friction coefficients as the flaked miniguide increases friction and the base texture decreases it.

Among the texture with the same dimple depth, it is possible to observe that textures with the medium or high proportion of plain surface are the ones that show best friction coefficients. When it comes to comparing textures with the same density, it is possible to see that greater dimple depth provides better friction coefficients with low and medium proportions of plain surface and smaller dimple depth is more beneficial when plain surface proportion increases. Table 7 shows the friction coefficient reductions of the different textures respect to the flaked surface.

	T1	T2	T3	T4	T5	T6 =TB
<b>0,1 Hz</b>	8	23	15	23	8	23
<b>1 Hz</b>	33	20	0	7	7	33
<b>7,5 Hz</b>	62	71	33	43	14	71
<b>15 Hz</b>	75	83	67	67	46	75

Table 7. Friction coefficient reductions of textures T1, T2, T3, T4, T5 and T6 vs the flaked surface.

Given this friction coefficient reductions it is possible to say that T2 is texture that has the best performance, especially because the improvement that shows for high displacement frequencies of the slides where flaking fails to keep values low. Hence, a textured surface that has deeper pockets and that keeps nearly the same proportion of texture and plain surface, provides the best friction properties for the guideways of the machine tool.

## 4. CONCLUSIONS AND FUTURE LINES

With the research developed a solution has been provided for a problem that up to now is solved in a manual way by means of flaking. Both a theoretical model and experimental tests have been presented using advanced technologies according to the current state of the art. The friction results obtained through tribological tests performed for the different textures that have been created, prove that texturing by grinding is an alternative with a greater potential than flaking for its application in the lubrication of the guideways in the machine tool sector. These competitive advantages translate into:

- Friction coefficient reduction of 8-23% in low frequencies and of 46-75% in high frequencies.
- Possibility to generate different textures in a controlled and repetitive way using the assisted dressing device and the texture generation and simulation model that have been developed. Prove of this are the results obtained in the confocal measurement, in which it is possible to observe that the textures obtained as a result are practically equal to the define (error in the depth of dimple is between 0 and 16% and error in density of the texture is 5-17%)
- Reduction of the time required to obtain the textures, since it is a completely automatized process, without increasing significantly the costs of the operation since grinding is already part of the manufacturing process of the guideways.

Given that the obtained results are positive, the future step is to introduce this technology in the real fabrication process of the guideways of the machine tools. This way, it would be possible to analyse whether this improvement of the frictional coefficient is translated into the improvement of the functioning of the machines, in relation to the obtained precision, observing effects such as the stick-slip or the behaviour of the guideways against wear.

## 5. ACKNOWLEDGMENTS

Thanks to the Basque Government for their support to this paper with the Research Project FAR (ZE-2018/00028).

## 6. REFERENCES

- [1] Lang AW, Motta P, Hidalgo P, Westcott M (2008) Bristled shark skin: a microgeometry for boundary layer control? *Bioinspiration & Biomimetics* Vol. 3 – 046005. DOI: 10.1088/1748-3182/3/4/046005.

- [2] Salaberry PC (2010) Vehicle with drag-reducing outer surface. U.S. Patent 7810867 B2.
- [3] Tagawa N, Bogy DB (2002) Air film dynamics for micro-textured flying head slider bearings in magnetic hard disk drives. *Journal of Tribology* Vol.124-3. p. 568-574. DOI: 10.1115/1.1456084
- [4] Kryzak Z, Pawlus P (2016) Zero-wear' of piston skirt surface topography. *Wear* Vol.260-4. p.554-561. DOI: 10.1016/j.wear.2005.03.038
- [5] Świrad S (2011) The surface texture analysis after sliding burnishing with cylindrical elements. *Wear* Vol.271-3. p.576-581. DOI: 10.1016/j.wear.2010.05.005
- [6] Holmberg K, Erdemir A (2017) Influence of tribology on global energy consumption, costs and emissions. *Friction* 5(3): 263–284. DOI: <https://doi.org/10.1007/s40544-017-0183-5>
- [7] Zhao B, Zhang S, Li J, Wang P (2016) Friction characteristics of sliding guideway material considering original surface functional parameters under hydrodynamic lubrication. *Proceedings of the Institution of Mechanical Engineers, Part J: Journal of Engineering Tribology* Vol.231. p.813-825. DOI: <https://doi.org/10.1177/1350650116681941>
- [8] Hsieh T.H, Jywe W.Y, Huang H.I, Chen S.L (2011) Development of a laser-based measurement system for evaluation of the scraping workpiece quality. *Optics and Lasers in Engineering* Vol.49. p.1045-1053. DOI: <https://doi.org/10.1016/j.optlaseng.2011.04.005>
- [9] Schneider Y.G (1984) Formation of surfaces with uniform micropatterns on precision machine and instruments parts. *Precision Engineering* Vol.6. p.219-225. DOI: [https://doi.org/10.1016/0141-6359\(84\)90007-2](https://doi.org/10.1016/0141-6359(84)90007-2)
- [10] Hou Y, Chen D, Zheng L (1985) Effect of surface topography of scraped machine tool guideways on their tribological behaviour. *Tribology international* Vol.18. p.125-129. DOI: [https://doi.org/10.1016/0301-679X\(85\)90054-4](https://doi.org/10.1016/0301-679X(85)90054-4)
- [11] Tönshoff H.K, Karpuschewski B, Mandrysch T, Inasaki I (1998) Grinding process achievements and their consequences on machine tools challenges and opportunities. *CIRP Annals* Vol.47 p.651-668. DOI: [https://doi.org/10.1016/S0007-8506\(07\)63247-8](https://doi.org/10.1016/S0007-8506(07)63247-8)
- [12] Xing Y, Deng J, Wu Z, Wu F (2017) High friction and low wear properties of laser textured ceramic surface under dry friction. *Optics and Laser Technology* Vol.93. p.24-32. DOI: <https://doi.org/10.1016/j.optlastec.2017.01.032>
- [13] Saeidi D, Meylan B, Hoffmann P, Wasmer K (2016) Effect of surface texturing on cast iron reciprocating against steel under starved lubrication conditions: A parametric study. *Wear* Vol.348-349. p.17-26. DOI: <https://doi.org/10.1016/j.wear.2015.10.020>
- [14] Wang D. W, Mo J. L, Zhu Z.Y, Ouyang H, Zhu M.H, Zhou Z.R (2018) Debris trapping and space-varying contact via surface texturing for enhance noise performance. *Wear* Vol.396-397. p.86-97. DOI: <https://doi.org/10.1016/j.wear.2017.11.013>
- [15] Bruzzone A.A.G, Costa H.L, Lonardo P.M, Lucca D.A (2008) Advances in engineered surfaces for frictional performance. *CIRP Annals – Manufacturing Technology* Vol.57. p.750-769. DOI: <https://doi.org/10.1016/j.cirp.2008.09.003>
- [16] Costa HL, Hutchings IM (2007) Hydrodynamic lubrication of textured steel surfaces under reciprocating sliding conditions. *Tribology International* Vol. 40. P.1227-1238. DOI: <https://doi.org/10.1016/j.triboint.2007.01.014>
- [17] Galda L, Pawlus P, Sep J (2009) Dimples shape and distribution effect on characteristics of Stribek curve. *Tribology International* Vol. 42-10. p.1505-1512. DOI: <https://doi.org/10.1016/j.triboint.2009.06.001>

- [18] Galda L, Dzierwa A, Sep J, Pawlus P (2010) The effect of oil pockets shape and distribution on seizure Resistance in Lubricated Sliding. *Tribology letters* Vol.37-2. p.301-311. DOI: 10.1007/s11249-009-9522-7
- [19] Nakano M, Korenaga A, Korenada A, Miyake K, Murakami T, Ando Y, Usami H, Sasaki S (2007) Applying Micro-Texture to Cast iron Surfaces to Reduce the Friction Coefficient Under Lubricated Conditions. *Tribology letters* Vol.28-2. p.131-137. DOI: 10.1007/s11249-007-9257-2
- [20] Kovalchenko A, Ajayi O, Erdemir A, Fensle G, Etsion I (2005) The effect of laser Surface texturing on transitions in lubrication regimes during unidirectional sliding contact. *Tribology International* Vol.38-3. p.219-225. DOI: <https://doi.org/10.1016/j.triboint.2004.08.004>
- [21] Stepien P, Szafarczyk M (1989) Generation of Regular Patterns on Ground Surfaces. *CIRP Annals* Vol.38-1. p.561-566. DOI: [https://doi.org/10.1016/S0007-8506\(07\)62769-3](https://doi.org/10.1016/S0007-8506(07)62769-3)
- [22] Stepien P, Balasz B (2006) Simulation of the formation process of regular grooves on the ground surface. *Proceedings of the fourth annual industrial simulation conference, Eurosis, Palermo* Vol. 269-276.
- [23] Stepien P (2006) Three Basic Types of Regular Surface Texture Generated by Plunge Grinding with the wheel having helical grooves. *Advances in Manufacturing Science and Technology* Vol.30-3. p.37-54.
- [24] Stepien P (2007) Grinding forces in regular surface texture generation. *International Journal of Machine Tools and Manufacture* Vol.45-14. p.2098-2110. DOI: <https://doi.org/10.1016/j.ijmachtools.2007.05.004>
- [25] Stepien P (2008) The mechanism of grinding wheel surface reproduction in regular Surface texture generation. *Surface Engineering* Vol.24-3. p.219-225. DOI: 10.1179/174329408X282596
- [26] Stepien P (2009) Regular Surface Texture Generated by Special Grinding Process. *Journal of Manufacturing Science* Vol. 131-1.
- [27] Denkena B, de Leon L, Wang B (2009) Grinding of microstructured functional surfaces: a novel strategy for dressing of microprofiles. *Production Engineering* Vol.3-1. p.41-48. DOI: 10.1007/s11740-008-0134-0
- [28] Denkena B, Kohler J, Wang B (2010) Manufacturing of functional riblet structures by profile grinding. *CIRP Journal of Manufacturing Science and Technology* Vol.3-1. p.14-26. DOI: <https://doi.org/10.1016/j.cirpj.2010.08.001>
- [29] Denkena B, Kästner J, Wang B (2010) Advanced microstructures and its production through cutting and grinding. *CIRP Annals – Manufacturing Technology* Vol.59 p.67-72. DOI: <https://doi.org/10.1016/j.cirp.2010.03.066>
- [30] Oliveira JFG, Bottene AC, Franca TV (2010) A novel dressing technique for texturing of ground surfaces. *CIRP Annals* Vol.59-1. p.361-364. DOI: <https://doi.org/10.1016/j.cirp.2010.03.119>
- [31] da Silva EJ, Oliveira JFG, Salles BB, Cardoso RS, Reis VRA (2019) Strategies for production of parts textured by grinding using patterned wheels. *CIRP Annals* Vol. 62-1. p.355-358. DOI: <https://doi.org/10.1016/j.cirp.2013.03.123>